Green Chemistry

Cite this: *Green Chem.*, 2012, **14**, 2017

www.rsc.org/greenchem

PAPER

Microemulsions with renewable feedstock oils

Michael L. Klossek, Didier Touraud and Werner Kunz*

Received 9th January 2012, Accepted 14th May 2012
DOI: 10.1039/c2gc35035a

In this paper we discuss the influence of chemical structures of renewable feedstock oils (RFOs) on the domains of existence and the nano-structures of microemulsions. We compare the results to those of classical microemulsions containing classical *n*-alkanes. First, the domains of microemulsions obtained from the melt of water, sodium dodecyl sulfate (SDS) as surfactant, 1-pentanol as co-surfactant and different RFOs (or RFO melts) in pseudo-ternary phase diagrams are presented. A surfactant–co-surfactant mass ratio of 1 : 2 is kept constant and the RFO (or RFO melt) is considered as a pseudo-constituent. Two different fatty methyl ester (FAME) biodiesels from rapeseed and cuphea oils, rapeseed oil, "TBK" biodiesel from rapeseed oil, limonene, and different mixtures of limonene to FAME-rapeseed biodiesel and FAME-rapeseed biodiesel to FAME-cuphea biodiesel are used as RFOs or RFO melts. Second, conductivity data are shown along an experimental path having a constant RFO or RFO melt : (surfactant–co-surfactant) mass ratio, whereas the water content is varied. All obtained data are then compared to data from previous studies with a series of *n*-alkanes (from *n*-hexane to *n*-hexadecane). As the main conclusion it is found that RFOs or RFO melts can easily substitute *n*-alkanes. From the chemical structure of the oils, it appears that not only the polarity of the oil plays an important role but also does the absolute size of the oil molecules. In all cases microemulsion systems exhibit percolative behavior.

1. Introduction

Microemulsions have attracted attention in science and industry for a long time. They show thermodynamic stability, optical clarity and high solubilization capacity,[1] and are isotropic with ultralow interfacial tension.[2,3] Usually, microemulsions are mixtures of non-polar solvents with polar liquids like water stabilized by a surfactant,[4,5] frequently in combination with a co-surfactant – often a short or medium chain alcohol[6] – forming an interfacial film that separates the two, in principle immiscible, solvents.[7] Though they are macroscopically homogeneous solutions, an ordered structure can be found on the nanoscopic scale such as oil-in-water (o/w) or water-in-oil (w/o) droplets, similar to the structures of micelles,[8–10] but with droplet sizes of 100 nm.[3] Besides droplets, lamellar,[11–13] random[14,15] or bicontinuous[3,16,17] microstructures, a network of water tubes in an oil matrix or a network of oil tubes in a water matrix have been identified. Various experimental methods like small angle neutron scattering (SANS),[18,19] neutron spin echo,[20] NMR,[21,22] freeze fracture electron microscopy (FFEM),[23] cryo-scanning electron microscopy,[24] and conductivity measurements[25] have been used to investigate these microstructures.

However, for a first screening, such sophisticated experiments are not necessary. The measurement of electrical conductivity is a very efficient method to study the global structure of microemulsions, especially in the case of w/o systems.[26,27] The electrical conductivity undergoes a significant change over many orders of magnitude when the volume fraction of the dispersed aqueous pseudo-phase is increased above a certain value. The sharp increase is a consequence of the percolative behavior of formed nanostructures in the system.[27] The percolation is induced when droplets in the microemulsion come close enough for ion exchange from one to another or when the droplets coalesce and form clusters leading to an exchange of material.[28] This phenomenon can be observed when the specific conductivity of the polar phase is some orders of magnitude higher than the one of the oil. Sometimes, anti-percolative behavior is observed. Then, only a small increase or even a decrease of conductivity is reported when increasing the water content. Anti-percolation behavior is associated with the formation of droplets having rigid interfacial films, thus preventing the reversed micelles from merging.[29]

Microemulsions have been intensively studied during the last few years by many scientists and technologists. The applications investigated at present range from classical fields like solubilization media in the food, cosmetic[30–33] and pharmaceutical industries,[34–37] oil recovery,[38] ground water remediation,[7,39] soil cleanup[40] and organic chemistry to new fields like improvement of fuels[5] or for use as decontamination media.[41] The use of microemulsions is not only advantageous due to the facile and

Institute of Physical and Theoretical Chemistry, University of Regensburg, 93040 Regensburg, Germany.
E-mail: werner.kunz@chemie.uni-regensburg.de;
Fax: +49 941 943 4532; Tel: +49 941 943 4044

low cost preparation, but also because of the improved bioavailability.[4,42]

Due to the consumer lifestyle of health and sustainability (LOHAS) requiring bio-based concepts it is a must to formulate and characterize microemulsions based on biological amphiphiles[43] and different kinds of renewable feedstock oils (RFOs).[5,37,44,45] Nowadays green microemulsions are already on the market.[32,42,43,46] Especially mono-alkyl esters made from renewable biological sources such as vegetable oils or animal fats have been investigated, and the physical properties of microemulsions with these compounds as the oil phase are of growing interest.[43,47–49]

Biodiesel is obtained by transesterification of vegetable oils with monohydric alcohols, commonly methanol, to give the corresponding mono-alkyl esters (FAME).[50,51] Besides sunflower, rapeseed, palm and soybean oil,[47,52,53] sources such as used cooking oils, jatropha[54] and algae[55] oils are receiving increasing attention. As early as in the 1960s, cuphea, with its vast diversity of fatty acids,[56,57] was proposed as a source of fatty acids with medium chain lengths.[58] In recent years, biodiesel has gained importance in a great number of research and industrial processes, for example as green solvents,[59–61] in cleaning and degreasing agents[62] or cleaning up of oil spills,[63] as polymerization solvents,[64] in pesticides[43,46,65] or as an alternative to organic solvents in liquid–liquid extractions[66] and last but not least as biofuels. Biodiesel based microemulsions have already been made and tested[41] and the produced bicontinuous microemulsion-fuels are effective fuels with low emissions.[67–69] It was shown that biodiesel from cuphea oil had improved fuel properties due to the composition of triglycerides,[70] a relatively high cetane number and a low cloud point.[57] Other advantages of biodiesel are the absence of aromatic hydrocarbons, low or no sulfur content and a positive energy balance. Some advantages in the use of FAME as green solvents in the formulation of microemulsions are their lower toxicity,[71–73] rapid biodegradability in soil,[74] low vapour pressure and non-inflammability.[75] The problems due to the over-production of glycerol induced by the classical processes of transesterification can be avoided by the production of "TBK" biodiesel. In this process triglycerides react with ethyl acetate, another green solvent, to give TBK-biodiesel associated with partially acetylated triglycerides.[76]

Another class of molecules widely used as solvents, and as a promising substitute for the oil compound in microemulsions, are monoterpenes. These are inexpensive monocyclic, monoterpenic hydrocarbons produced from renewable feedstock and the major constituents of citrus oils.[77] Limonene itself is among the most commonly used fragrance additives or active substances in technical and fine products, for example in defatting agents,[78] cleaners,[79] in perfumes, soaps, foods and beverages, with a typical concentration between 50 ppm and 2300 ppm,[78] and it can be used as a fuel or fuel additive[80,81] as well. Microemulsions based on limonene are of great importance in the formulation, for example, of pharmaceuticals,[4,82] cleaning agents,[83,84] and flavouring vectors in foods and beverages[85] *etc.* Anti-carcinogenic properties[86] have been shown and limonene is considered to be a skin irritant and a sensitizer in high concentrations,[87] but not allergenic.[88]

The main purpose of the present article is to compare the influence of the use of RFOs and non-renewable feedstock oils (NRFOs) in order to formulate microemulsions. The domain of existence and the nano-structures of microemulsions with different RFOs or RFO melts, and NRFOs ranging from hexane to hexadecane are then compared using ternary phase diagrams and conductivity measurements; sodium dodecyl sulfate (SDS) and 1-pentanol are used respectively as surfactant and co-surfactant. The used RFOs or RFO melts are two different FAME (fatty methyl ester) biodiesels from rapeseed and cuphea oil, TBK biodiesel from rapeseed oil, limonene, and mixtures of limonene and FAME-rapeseed biodiesel as well as FAME-rapeseed and FAME-cuphea biodiesel. The biodiesels essentially differ in the carbon chain length and proportion of unsaturation of the fatty methyl esters and the amounts of tri-, di- and mono-glycerides.

2. Experimental

2.1. Materials

All solutions were prepared with water with a resistivity of 18.2 mΩ cm^{-2}. Sodium dodecyl sulfate $\geq$ 99.0%, 1-pentanol $\geq$ 98% and *R*-(+)-limonene $\geq$ 94% were purchased from Merck KGaA (Darmstadt, Germany). The FAME-rapeseed biodiesel and the TBK rapeseed biodiesel were generous gifts respectively from Tecosol (Ochsenfurt, Germany) and Mr János Thész (Hungary), and the FAME-cuphea biodiesel was kindly prepared for us by Dr Gerhard Knothe from the National Center for Agricultural Utilization Research (Peoria, Illinois, USA). Rapeseed oil was purchased from VOG AG (Linz, Austria). All the chemicals were used without further purification.

2.2. Methods and techniques

Phase diagrams. Systems consisting of water, RFO or RFO melt, surfactant and co-surfactant melt can be described within a pseudo-ternary phase diagram, see Fig. 1. As a reference system, water/*n*-alkane/sodium dodecyl sulfate/1-pentanol was chosen with the surfactant to co-surfactant ratio kept constant (1 : 2 in mass ratio) (see Fig. 1). These diagrams were established as described in the following section and according to ref. 89.

In screwable tubes a mixture of emulsifiers containing always the same proportions of surfactant : co-surfactant was blended with RFO, RFO melt or water at determined weight ratios to obtain a starting weight of 3 g. Water (RFO or RFO melt) was

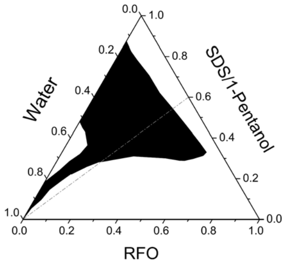

Fig. 1 Illustration of a pseudo-ternary phase diagram (in weight fractions) with water/SDS/1-pentanol/RFO. Additionally, the pathway on which all conductivity measurements were performed is shown. The weight ratio of oil : surfactant–co-surfactant was kept constant at 0.4.

added with Eppendorf pipettes to the resulting mixture until a change in the phase occurs. Besides microemulsions, the formation of liquid crystalline phases, "classical" emulsions and a homogeneous solution in equilibrium with undissolved SDS can occur. The different phases were determined with the naked eye and with the help of polarizing filters in order to discern the homogeneous liquid crystalline phases of the microemulsions. Under polarizing filters most of the liquid crystalline phases appear birefringent. The amount of added water (RFO or RFO melt) was recorded. The temperature was kept constant at 25 °C with a thermostatically controlled test tube rack.

Conductivity. Conductivity measurements were carried out at 25 °C with the inoLab®Vario Cond 730 Conductometer. The temperature was controlled by a thermostated cell. All measurements were conducted twice. The experimental error is approximately 2.5%. RFO, RFO melt or *n*-alkane based w/RFO or RFO melt microemulsions were prepared as described above whereas the content of water was as low as possible. Water was then progressively added with an Eppendorf pipette and the volume and the corresponding specific conductivity were recorded. The measurement was finished when the turbid area was reached. The experimental path is shown in Fig. 1.

3. Results and discussion

3.1. Phase diagrams

FAME-rapeseed biodiesel and limonene – two "green" solvents. At first, FAME-rapeseed biodiesel, limonene and afterwards melts of those RFOs were used as the oil phase. For this purpose, the phase diagrams for the limonene to biodiesel melt with biodiesel to limonene mass ratios of 1 : 3, 1 : 1 and 3 : 1 were also determined. The resulting phase diagrams are illustrated in Fig. 2. The black areas represent the clear and homogeneous single phase regions without liquid crystals. These areas can be assimilated to the domain of existence of microemulsions.[64]

The use of limonene gives a phase diagram with two domains of existence of microemulsions, L1 and L2, as in the case where *n*-hexane or *n*-heptane are used, see Fig. 3. L1 is constituted of oil-in-water droplets for the compositions having the highest proportions of water. In L1, the microemulsions can have a high content of oil. Then, they can be bicontinuous or still form oil-in-water droplets. The exact determination of the structure of these microemulsions remains a matter of discussion, and is not the motivation of the present paper. L2 is formed by reversed water-in-oil droplets at low water contents. A more detailed discussion concerning the evolution of the structures of the L2 domain, increasing the water content, is planned later. L1 and L2 are generally separated by clear or unclear, or homogeneous or non-homogeneous media showing liquid crystalline phases. The area between L1 and L2 generally contains liquid crystals (LC).

The domain of existence of the microemulsions obtained using FAME-rapeseed biodiesel is more like the one observed in the presence of *n*-hexadecane. The phase diagram shows a microemulsion domain that consists of a large single realm of existence comparable to the domains obtained with long-chain *n*-alkanes, see Fig. 3. In this case the water-in-oil droplets obtained at low water contents can be converted into oil-in-water droplets by adding water along some well-defined paths that do not pass through the LC area. The structure of the microemulsions between the water-in-oil and the oil-in-water droplets is then bicontinuous. By mixing both RFOs, it is possible to screen roughly the whole spectrum of pseudo-ternary phase diagrams with conventional alkanes, beginning with *n*-octane and ending with *n*-hexadecane. For the mixtures of both RFOs however, slight differences of phase behaviors in comparison to the ones obtained with *n*-alkanes are apparent. The main difference appears for the domains of existence of microemulsions obtained with the weight ratio 1 : 1 of limonene to FAME-rapeseed biodiesel. In particular, the appendix (noted Ap in Fig. 2, diagram (iii)) appears less extended than in the case of the use of *n*-decane or *n*-undecane (Fig. 3, diagrams (d) and (e)). The loss of this appendix can be explained by the formation of microemulsions due to the increased flexibility of the *n*-alkane

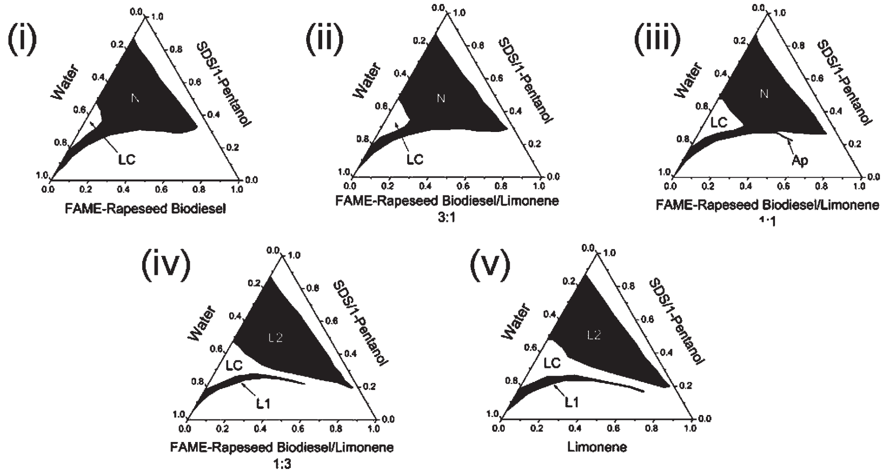

Fig. 2 Pseudo-ternary phase diagrams for the system water/SDS/1-pentanol/RFO at 25 °C and constant weight ratio of SDS to 1-pentanol (1 : 2) with (i) FAME-rapeseed biodiesel, (ii) FAME-rapeseed biodiesel : limonene 3 : 1, (iii) FAME-rapeseed biodiesel : limonene 1 : 1, (iv) FAME-rapeseed biodiesel : limonene 1 : 3 and (v) limonene as RFO phase. Compositions are in weight ratio.

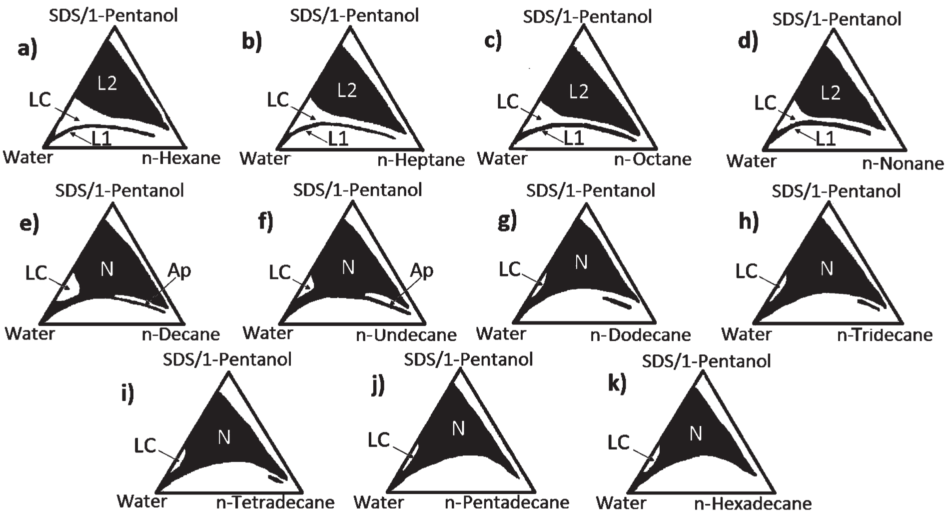

Fig. 3 Homologous series of pseudo-ternary phase diagrams for the water/SDS/1-pentanol/*n*-alkanes systems. The domains of existence of the microemulsions are represented in black. All these phase diagrams were determined during previous work[90] using the same method as described in the section "Methods and techniques". Temperature was kept constant at 25 °C and the weight ratio of SDS to 1-pentantol (1 : 2) as well.

molecules. Nevertheless, the main microemulsion domains are similar to those found for the homologous series of the *n*-alkanes (Fig. 3) considering an increase of the average number of carbon atoms or an increase of the average volume per RFO and *n*-alkane molecules from limonene to FAME-rapeseed biodiesel and from *n*-hexane to *n*-hexadecane.

FAME, TBK rapeseed biodiesel, FAME-cuphea biodiesel and rapeseed oil – a comparison. In the next step, the domains of existence of microemulsions using as RFOs TBK-rapeseed biodiesel and FAME-cuphea biodiesel are determined. Fig. 4 shows the resulting phase diagrams. For a better comparison, the diagram water/SDS/1-pentanol/FAME-rapeseed biodiesel (2(i)) is again reported.

For TBK-rapeseed oil a large single realm of existence N is observed and the topology of the phase diagram is similar to that observed with hexadecane (Fig. 3(k)). In the case of the FAME-rapeseed diagram, the extent of the homogeneous transparent N phase into the oil-rich region is less pronounced. This may be explained by the lack of mono- and diglycerides, which are widely present in the TBK-rapeseed system and which exhibit a much stronger propensity to the interface than triglycerides.

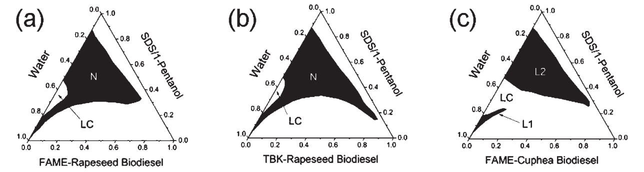

Fig. 4 Influence of different types of biodiesel on the domain of existence of microemulsions for the system water/SDS/1-pentanol: (a) FAME-rapeseed biodiesel, (b) TBK-rapeseed biodiesel and (c) FAME-cuphea biodiesel. Temperature was kept constant at 25 °C.

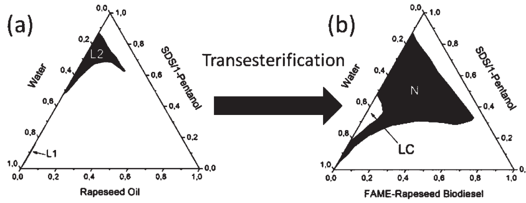

Fig. 5 Influence of the production of FAME on the solubilisation of the renewable carbon coming from the rapeseed oil: (a) pseudo-ternary phase diagram of the system water/SDS/1-pentanol/rapeseed oil and (b) pseudo-ternary phase diagram of the system water/SDS/1-pentanol/FAME-rapeseed biodiesel at 25 °C and at a constant weight ratio of SDS to 1-pentanol (1 : 2).

Biodiesel derived from cuphea oil leads to two separate L1 and L2 domains, but the extent of L1 towards the oil area is more limited in comparison to the ones obtained using short-chain *n*-alkanes or limonene. Nevertheless, the presence of the two domains L1 and L2 is in agreement with the fact that the molecular structures of the fatty acid mono-alkyl esters of the FAME-cuphea biodiesel have a number of carbon atoms and a molecular volume closer to short-chain *n*-alkanes than to long-chain ones. From cuphea seed especially saturated fatty acids with medium chain lengths of C8–C16 are achieved, with decanoic acid being one of the main fatty acids (about 60% of total fatty acid contents in most cuphea species[56,57,86]). The reduction of the L1 domain of microemulsions could be due to a reduction of the flexibility of the FAME-cuphea biodiesel molecules. This can be attributed to a slight co-surfactant behavior of the ester-group leading to a greater interaction with the 1-pentanol/SDS bilayer.

Now we compare the phase diagram obtained with pure rapeseed oil to the phase diagram based on FAME-rapeseed biodiesel in order to investigate the influence of the transesterification reaction on the extent of the domain of existence of microemulsions, see Fig. 5.

The used FAME-biodiesel was produced by transesterification of rapeseed oil with methanol, to give the corresponding mono-alkyl esters (FAME). It appears that this reaction is largely favorable for the formation of microemulsions. As the fatty acids are also linked to the glycerol by ester-functions, the polarities of the rapeseed oil molecules and of the FAME molecules should be comparable. So it seems that the number of carbon atoms per molecule or the molecular volume is the decisive parameter which makes the difference in the phase behaviours and not the polarity of the oil molecules. Fig. 6 shows that similar to limonene, FAME-cuphea biodiesel can roughly yield the whole spectrum of pseudo-ternary phase diagrams known from alkanes beginning with *n*-octane and ending with *n*-hexadecane, by mixing it with appropriate amounts of FAME-rapeseed biodiesel.

3.2. Conductivity

Independently of the oil components, all the microemulsion systems exhibit a similar general dependence of the electrical conductivity on the amount of water (see Fig. 7). At low water content, the electrical conductivity of the samples is close to zero, which can be attributed to the fact that the oils forming the initial continuous pseudo-phase constitute an excellent insulator to the first reversed water in oil droplets formed. Then, there is a progressive increase in electrical conductivity with increasing amounts of water.

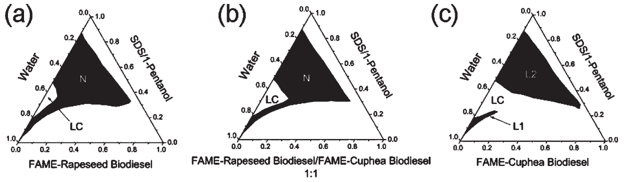

Fig. 6 Pseudo-ternary phase diagrams for the system water/SDS/1-pentanol/RFO at 25 °C and a constant weight ratio of SDS to 1-pentanol (1 : 2) with (a) FAME-rapeseed biodiesel, (b) FAME-rapeseed biodiesel : FAME-cuphea biodiesel 1 : 1, and (c) FAME-cuphea biodiesel as RFO phase.

This well-known behavior can be explained with a percolation model.[26,91] At the percolation threshold, the water-in-oil droplets form nano-clusters favorable to the SDS counter-ion mobility. The deviation from the linearity observed for higher water content in the presence of certain oils has been ascribed to the formation of bicontinuous structures, generally observed before the pseudo-phase inversion. The percolation threshold (value of the water content where a large increase of the conductivity value starts) appears to be dependent on the chemical nature of the oil. The more the oils have molecules with a high average number of carbon atoms (or a high molecular volume), the lower is the value of the percolation threshold. In Fig. 7 it can be seen that the curves obtained in the presence of *n*-hexadecane and *n*-hexane are the upper and lower boundaries, respectively, and the other curves are situated in between. The conductivity curves obtained using TBK- and FAME-rapeseed biodiesel are close to the one obtained with *n*-hexadecane whereas those obtained using FAME-cuphea biodiesel or limonene are in the vicinity of the one recorded in the presence of *n*-hexane. This result is in line with the observations concerning the domains of existence of microemulsions in the pseudo-ternary phase diagrams (previous section). The conductivity curves obtained from melts of FAME-rapeseed biodiesel and limonene show the same trend (see Fig. 7(b)). With increasing amounts of FAME-rapeseed biodiesel, there is a shift of the percolation towards lower values. The curves obtained using the FAME-rapeseed biodiesel only (oil with a higher average number of carbons per molecule) and the limonene (oil with a lower number of carbons per molecule) are the lower and upper curves and all the other curves are in between, in the expected order.

4. Conclusions

This study shows the possibility of replacing classical *n*-alkanes as the oil phase in common microemulsions by green RFOs, whether RFOs are "pure" or a mixture of RFOs of different

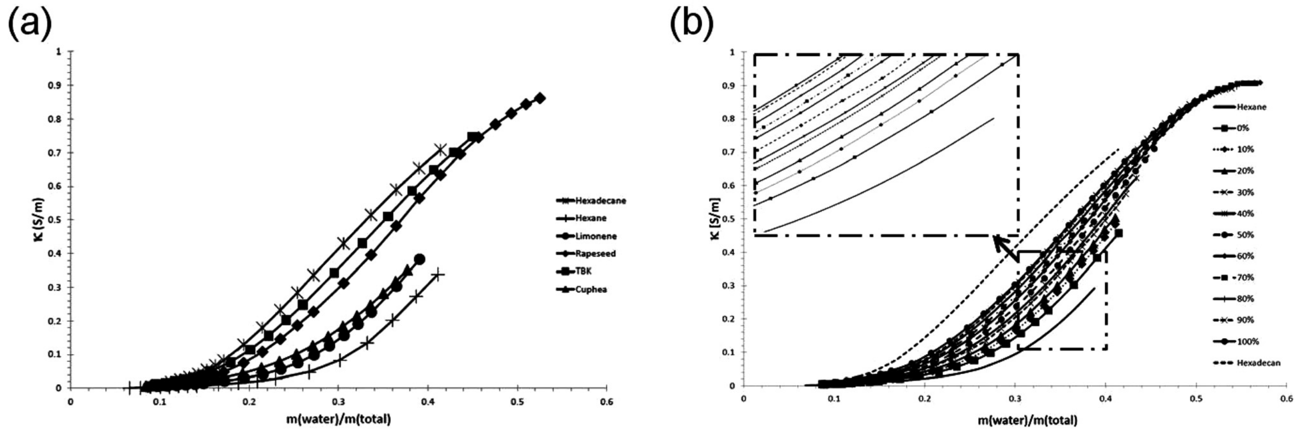

Fig. 7 (a) The specific conductivity of the microemulsions as a function of water weight ratio for the pseudo-ternary system water/SDS/1-pentanol/oil with a constant weight ratio of SDS to 1-pentanol (1 : 2) is shown. As the oil phase either hexadecane, or hexane, or limonene, or FAME-rapeseed, or TBK-rapeseed, or FAME-cuphea biodiesels were used. (b) The specific conductivity of the microemulsions as a function of water weight content for the pseudo-ternary system water/SDS/1-pentanol/oil with a constant weight ratio of SDS to 1-pentanol (1 : 2) is shown. As the oil phase mixtures of FAME-rapeseed biodiesel and limonene were used. The experimental path of the conductivity measurements is the same as already shown and explained in Fig. 1. All experiments were recorded at 25 °C.

origins. Limonene and cuphea biodiesel can replace short-chain alkanes whereas TBK- and FAME-rapeseed biodiesel can substitute long-chain ones (see Fig. 1). The extent of the microemulsion domains and the organization of the nano-droplets can be predicted by the average number of carbons per molecule (or the average molecular volume) of the RFO or RFO mixtures. The presented results may be used to formulate more environmentally friendly industrial products, *e.g.* "green" cutting fluids, such as pesticides,[43] cosmetics[31,32] or pharmaceuticals.[41] Furthermore, from the phase diagrams shown in the present work (Fig. 2(ii, iii), Fig. 6(b)) the formulation of a potential bicontinuous microemulsion-fuel of FAME-rapeseed biodiesel and FAME-cuphea biodiesel (or limonene) mixtures appears possible. By the addition of cuphea biodiesel (or limonene), a lower cloud point of the system and a positive influence on the combustion could be expected.

All these systems show percolative behavior, whatever the molecular volume or the polarity of the oil. This result is in agreement with the fact that the passage to an anti-percolative system depends rather on the nature of the alcohol used as co-surfactant than on the nature of the oil; the longer chain alcohols are responsible for the appearance of anti-percolative behavior.[89]

References

1 V. Papadimitriou, S. Pispas, S. Syriou, A. Pournara, M. Zoumpanioti, T. G. Sotiroudis and A. Xenakis, *Langmuir*, 2008, **24**, 3380–3386.
2 L. Do, A. Withayyapayanon, J. Harwell and D. Sabatini, *J. Surfactants Deterg.*, 2009, **12**, 91–99.
3 Y. Gao, S. Wang, L. Zheng, S. Han, X. Zhang, D. Lu, L. Yu, Y. Ji and G. Zhang, *J. Colloid Interface Sci.*, 2006, **301**, 612–616.
4 C.-H. Liu, F.-Y. Chang and D.-K. Hung, *Colloids Surf., B*, 2011, **82**, 63–70.
5 A. Kogan and N. Garti, *Adv. Colloid Interface Sci.*, 2006, **123**, 369–385.
6 M. Kahlweit, R. Strey, D. Haase, H. Kunieda, T. Schmeling, B. Faulhaber, M. Borkovec, H.-F. Eicke, G. Busse, F. Eggers, T. Funck, H. Richmann, L. Magid, O. Söderman, P. Stilbs, J. Winkler, A. Dittrich and W. Jahn, *J. Colloid Interface Sci.*, 1987, **118**(2), 436–453.
7 S. Wellert, M. Karg, H. Imhof, A. Steppin, H.-J. Altmann, M. Dolle, A. Richardt, B. Tiersch, J. Koetz, A. Lapp and T. Hellweg, *J. Colloid Interface Sci.*, 2008, **325**, 250–258.
8 T. P. Hoar and J. H. Schulman, *Nature*, 1943, **152**, 102–103.
9 H. Gao, J. Li, B. Han, W. Chen, J. Zhang, R. Zhang and D. Yan, *Phys. Chem. Chem. Phys.*, 2004, **6**, 2914–2916.
10 J. L. Anderson, J. Ding, T. Welton and D. W. Armstrong, *J. Am. Chem. Soc.*, 2002, **124**, 14247–14254.
11 H. Saito and K. Shinoda, *J. Colloid Interface Sci.*, 1970, **32**, 647.
12 K. Shinoda and S. Friberg, *Adv. Colloid Interface Sci.*, 1975, **4**, 281–300.
13 K. Shinoda, *Prog. Colloid Polym. Sci.*, 1983, **68**, 1.
14 Y. Talmon and S. Prager, *J. Chem. Phys.*, 1978, **69**, 2984.
15 J. Jouffray, P. Levinson and P. DeGennes, *J. Phys.*, 1982, **43**, 1241.
16 L. E. Scriven, *Nature*, 1976, **263**, 123–125.
17 D. Langevin, *Annu. Rev. Phys. Chem.*, 1992, **43**, 341–369.
18 H. Endo, M. Mihailescu, M. Monkenbusch, J. Allgaier, G. Gompper, D. Richter, B. Jakobs, T. Sottmann, R. Strey and I. Grillo, *J. Chem. Phys.*, 2001, **115**, 580–600.
19 F. Lichterfeld, T. Schmeling and R. Strey, *J. Phys. Chem.*, 1986, **90**, 5762–5766.
20 M. Mihailescu, M. Monkenbusch, H. Endo, J. Allgaier, G. Gompper, J. Stellbrink, D. Richter, B. Jakobs, T. Sottmann and B. Farago, *J. Chem. Phys.*, 2001, **115**, 9563–9577.
21 B. Lindman, N. Kamenka, T. M. Kathopoulis, B. Brun and P. G. Nilsson, *J. Phys. Chem.*, 1980, **84**, 2485–2490.
22 J. F. Bodet, J. R. Bellare, H. T. Davis, L. E. Scriven and W. G. Miller, *J. Phys. Chem.*, 1988, **92**, 1898–1902.
23 S. Burauer, L. Belkoura, C. Stubenrauch and R. Strey, *Colloids Surf., A*, 2003, **228**, 159–170.
24 C. Note, J. Ruffin, B. Tiersch and J. Koetz, *J. Dispersion Sci. Technol.*, 2007, **28**, 155–164.
25 M. Dvolaitzky, M. Lagues, J. P. L. Pesant, R. Ober, C. Sauterey and C. Taupin, *J. Phys. Chem.*, 1980, **84**, 1532–1535.
26 B. Lagourette, J. Peyrelasse, C. Boned and M. Clausse, *Nature*, 1979, **281**, 60–63.
27 M. Lagues, *J. Phys., Lett.*, 1979, **40**, 331.
28 P. Alexandridis, J. F. Holzwarth and T. A. Hatton, *J. Phys. Chem.*, 1995, **99**, 8222–8232.
29 T. Zemb, *Colloids Surf., A*, 1997, **129**, 435–454.
30 *Microemulsions in Cosmetic, in Industrial Applications of Microemulsions*, ed. C. Solans and S. Solans, Marcel Dekker, New York, 1997.
31 M. H. W. von Rybinski and I. Johansson, Microemulsions in Cosmetics and Detergents, in *Microemulsions: Background, New Concepts, Application, Perspectives*, John Wiley & Sons Ltd, Chichester, 2009.
32 M. Hloucha, H.-M. Haake and G. Pellon, *Cosmet Toilet.*, 2009, **124**, 58.
33 http://www.cognis.com/company/Businesses/Care+hemicals/Products+and+concept+innovations/personal+care/Plantasil.htm
34 M. Lawrence and G. D. Rees, *Adv. Drug Delivery Rev.*, 2000, **45**, 89–121.
35 B. Paul and S. P. Moulik, *Curr. Sci.*, 2001, **80**, 990–1001.
36 N. Garti, *Curr. Opin. Colloid Interface Sci.*, 2003, **8**, 197–211.
37 J. Flanagan and H. Singh, *Crit. Rev. Food Sci. Nutr.*, 2006, **46**, 221–237.
38 T. Sottmann and C. Stubenrauch, *Microemulsions: Background, New Concepts, Application, Perspectives*, Blackwell Publishing Ltd, 2009.
39 J. H. Harwell, D. A. Sabatini and R. Knox, *Colloids Surf., A*, 1999, **151**, 255–268.
40 S. Jayanti, L. N. Britton, V. Dwarakanath and G. A. Pope, *Environ. Sci. Technol.*, 2002, **36**, 5491–5497.
41 S. Wellert, H. Imhof, M. Dolle, H.-J. Altmann, A. Richardt and T. Hellweg, *Colloid Polym. Sci.*, 2008, **286**, 417–426.
42 http://www.cognis.com/company/Businesses/agroSolutions/microemulsions
43 http://www.cognis.com/NR/rdonlyres/2101DE9F8DE0-4A0E-95BA-D3D1E3735080/0/Cognis_APG_Broschure_USA.pdf
44 D. A. Sabatini, R. C. Knox, J. H. Harwell and B. Wu, *J. Contam. Hydrol.*, 2000, **45**, 99–121.
45 J. D. Childs, E. Acosta, R. C. Knox, J. H. Harwell and D. A. Sabatini, *J. Contam. Hydrol.*, 2004, **71**, 27–45.
46 C.-P. Chin, C.-W. Lan and H.-S. Wu, *Ind. Eng. Chem. Res.*, 2012, **51**, 4710–4718.
47 K. Hill, *Pure Appl. Chem.*, 2000, **72**, 1255–1264.
48 T. N. deCastro Dantas, A. da Silva and A. Neto, *Fuel*, 2001, **80**, 75–81.
49 E. J. Silva, M. E. D. Zaniquelli and W. Loh, *Energy Fuels*, 2007, **21**, 222–226.
50 F. Ma and M. A. Hanna, *Bioresour. Technol.*, 1999, **70**, 1–15.
51 G. Knothe and K. R. Steidley, *Ind. Eng. Chem. Res.*, 2011, **50**, 4177–4182.
52 *The Biodiesel Handbook*, ed. G. Knothe, J. V. Gerpen and J. Krahl, AOCS Publishing, 2005.
53 *Biodiesel: The Comprehensive Handbook*, ed. M. Mittelbach and C. Remschmidt, Martin Mittelbach, 2006.
54 N. Foidl, G. Foidl, M. Sanchez, M. Mittelbach and S. Hackel, *Bioresour. Technol.*, 1996, **58**, 77–82.
55 Y. Chisti, *Biotechnol. Adv.*, 2007, **25**, 294–306.
56 R. Wolf, S. Graham and R. Kleiman, *J. Am. Oil Chem. Soc.*, 1983, **60**, 103–104.
57 G. Knothe, S. C. Cermak and R. L. Evangelista, *Energy Fuels*, 2009, **23**, 1743–1747.
58 T. W. T. Miwa and C. Smith, *J. Am. Oil Chem. Soc.*, 1960, **37**, 675–676.
59 J. Hu, Z. Du, Z. Tang and E. Min, *Ind. Eng. Chem. Res.*, 2004, **43**, 7928–7931.
60 J. H. Clark and S. J. Tavener, *Org. Process Res. Dev.*, 2007, **11**, 149.
61 F. M. Kerton, *Alternative Solvents for Green Chemistry*, RSC, Cambridge, UK, 2009, ch. 5.
62 S. Wildes, *Chem. Health Saf.*, 2002, **5/6**, 24.
63 N. Miller and S. M. Mudge, *Spill Sci. Technol. Bull.*, 1997, **4**, 17–33.
64 S. Salehpour and M. A. Dubé, *Green Chem.*, 2008, **10**, 321–326.
65 S. Salehpour, M. A. Dubé and M. Murphy, *Can. J. Chem. Eng.*, 2009, **87**, 129–135.
66 S. K. Spear, S. T. Griffin, K. S. Granger, J. G. Huddleston and R. D. Rogers, *Green Chem.*, 2007, **9**, 1008–1015.
67 R. Strey, A. Nawrath and T. Sottmann, US 2007/0028507 A1.
68 L. Bemert, S. Engelskirchen, C. Simon and R. Strey, *Prepr. Pap.-Am. Chem. Soc., Div. Fuel Chem.*, 2009, **54**, 290–291.

69 R. Strey, T. Sottmann, A. Nawrath, K. Rottländer, L. Bemert and S. Engelskirchen, WO 2010/133627 A2.

70 D. P. Geller, J. W. Goodrum and S. J. Knapp, *Ind. Crops Prod.*, 1999, **9**, 85.

71 N. Khan, M. Warith and G. Luk, *J. Air Waste Manage. Assoc.*, 2007, **57**, 286–296.

72 J. A. DeMello, C. Carmichael, E. E. Peacock, R. Nelson, J. S. Arey and C. M. Reddy, *Mar. Pollut. Bull.*, 2007, **54**, 894–904.

73 E. Dinjus, U. Arnold, N. Dahmen, R. Höfer and W. Wach, *Sustainable Solutions for Modern Economies, Chapter 8 Green Fuels – Sustainable Solutions for Transportation*, RSC, Cambridge, UK, 2009.

74 B. Vrana, G. A. Mills, E. Dominiak and R. Greenwood, *Environ. Pollut.*, 2006, **142**, 333–343.

75 Y. M. Gonzalez, P. de Caro, S. Thiebaud-Roux and C. Lacaze-Dufaure, *J. Solution Chem.*, 2007, **36**, 437–446.

76 J. Thész, B. Boros and Z. Király, WO 2008/096187 A1.

77 J. Sun, *Altern. Med. Rev.*, 2007, **12**, 259–264.

78 M. Matura, A. Goossens, O. Bordalo, B. Garcia-Bravo, K. W. K. Magnusson and A. T. Karlberg, *J. Am. Acad. Dermatol.*, 2002, **47**, 709–714.

79 http://www.ppiatlanta.com/pdfs/DataSheets/D-Limonene-%20uses.pdf

80 J. S. Willkins, US5575822, 1996.

81 T. Li, CN 101319146 (A), 2008-12-10.

82 M. Fanun, *Household Personal Care*, 2011, **2**, 10–12.

83 J. Drapier, M. Galvez, N. Kerzmann and G. Jakubicki, US 6048834.

84 http://www.airproducts.com/~/media/Downloads/Other/i-and-i-formulary%20brochure.ashx

85 C. Jameson, Toxicology and Carcinogenesis Studies of d-Limonene, *U.S. Department of Health and Human Services Technical Report NIH Publication No. 90-2802*, 1990.

86 P. L. Crowell and M. N. Gould, *Crit. Rev. Oncog.*, 1994, **5**, 1–22.

87 H. Okabe, Y. Obata, K. Takayama and T. Nagai, *Drug Des. Discov.*, 1990, **6**, 229–238.

88 A.-T. Karlberg, A. Boman and B. Melin, *Ann. Occup. Hyg.*, 1991, **35**(4), 419–426.

89 M. Clausse, L. Nicolas-Morgantini, A. Zradba and D. Touraud, *Surfactant Science Series, Microemulsion Systems*, Dekker, New York, 1987, vol. 24, p. 15.

90 D. Touraud, PhD thesis, Compiégne, 1991.

91 M. Clausse, J. Peyrelasse, J. Heil, C. Boned and B. Lagourette, *Nature*, 1981, **293**, 636–638.